ELSEVIER

Journal of Luminescence 91 (2000) 147–153

JOURNAL OF LUMINESCENCE

www.elsevier.com/locate/jlumin

Temperature-dependent spectroscopic analysis of F_2^+** and F_2^+**-like color centers in LiF

Neil W. Jenkins[a,*], Sergey B. Mirov[a], Vladimir V. Fedorov[b]

[a] *Laser & Photonics Research Center, Department of Physics, University of Alabama at Birmingham, Birmingham, AL 35294-1170, USA*
[b] *Research Center for Laser Materials & Technology, General Physics Institute, RAS, 38 Vavilov Street, Moscow 117942, Russia*

Received 19 October 1999; received in revised form 8 February 2000; accepted 4 April 2000

Abstract

A temperature-dependent spectroscopic analysis of the color center laser medium, LiF : F_2^+**, is shown. Special attention is devoted to the well-known F_2^+** color center as well as a new F_2^+**-like color center, conclusively discovered in this work, which is found to have a peak absorption near $\lambda^0_{abs} = 808$ nm and peak emission near $\lambda^0_{ems} = 1080$ nm. Justification for the association of this new center with F_2^+**-like color centers is explained in the text. Standard F_2^+** color centers have kinetics of fluorescence lifetime of $\tau_{13\,K} = 32$ ns, $\tau_{300\,K} = 21$ ns, for a quantum efficiency of fluorescence, $\eta = 66\%$. Concerning the new F_2^+**-like color center, the 13 K lifetime was found to be $\tau \approx 5$ ns. We show that Alexandrite laser radiation can simultaneously excite the absorption bands of both F_2^+**-like centers in their region of spectral overlap. The resulting emission from both centers is the mechanism responsible for the ultrabroadband range of tunability, ~800–1300 nm, from this laser medium at RT. This crystal is the heart of a potential ultrabroadband, near-IR laser; frequency doubling this fundamental output will realize a truly white-light laser.

PACS: 42.55.Qy; 42.60.Fc; 42.60.Jf; 78.50.Ec; 78.55.Hx

Keywords: Tunable lasers; LiF : F_2^+**; Color center lasers; Spectroscopic data

1. Introduction

The LiF : F_2^+** color center laser, which is both thermal- and photo-stable, has been shown to have high energy output (~100 mJ) and good efficiency (~tens of %) [1]. Also, the spectral output in Ref. [1] was shown to be very wide (796–1210 nm); however, reasonable explanations of such ultrabroadband tuning capability were not provided. The information addressed within this paper details the spectroscopic properties of the LiF : F_2^+** color center laser crystal, in particular, the F_2^+** and a new F_2^+**-like color centers, conclusively discovered in this study. We also illustrate in this paper that the absorption spectra (and thus the fluorescence spectra) of these centers overlap in a spectral region easily excited by radiation from an Alexandrite laser. Pumping

*Correspondence address. Present address: US Naval Research Laboratory, Code 5654, Washington, DC 20375, USA. Tel.: +1-202-767-9407; fax: +1-202-404-7530.

E-mail addresses: njenkins@phy.uab.edu, njenkins@ccsalpha3.nrl.navy.mil (N.W. Jenkins).

0022-2313/00/$ - see front matter
PII: S0022-2313(00)00228-3

within this region allows for simultaneously induced population inversion of both centers. This overlapping will be shown as the mechanism that accounts for the ultrabroad range of tunability.

2. Experimental results

Using a crystal sample from a single boule prepared by the method described in Ref. [2], the first measurements performed were of the transmission spectra of $LiF:F_2^+$**. A Shimadzu UV3101-PC spectrophotometer was used to perform these measurements. Initially, measurements at room temperature (RT) were performed; after those were completed, a Janis Research Co, Inc., Model CCS-450 closed cycle refrigerator system was utilized for measuring transmission at low temperatures. The crystal has thickness equal to 0.53 cm and was codoped with oxygen ($\sim 2\times 10^{17}\,cm^{-3}$), hydroxyl groups ($\sim 2\times 10^{18}\,cm^{-3}$), and Mg ($\sim 10^{17}\,cm^{-3}$).

Fig. 1 shows the RT absorption spectrum with corresponding coefficients, as well as a spectrum deconvolution of known color centers in the sample.

Fig. 2 shows a magnified view of the frequency region of interest, namely the region which contains the absorption curves of both F_2^+** and the new F_2^+**-like color centers. Similar F_2^+**-like absorption bands were presented by Ter-Mikirtychev in Ref. [3]; however, the fluorescence properties of the F_2^+**-like centers in Ref. [3] and those discussed in this paper are completely different.

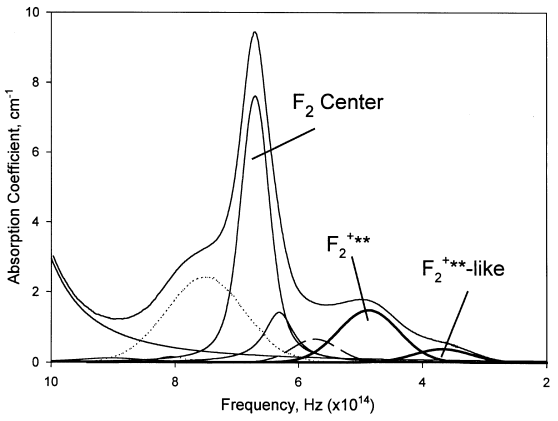

Fig. 1. Absorption spectrum and color center deconvolution at 300 K.

Deconvolution of these spectra shows that both the F_2^+** and F_2^+**-like color centers are best described by Gaussian lineshape functions and have properties described in Table 1.

Absorption measurements at 13 K were also performed on the same sample. Figs. 3 and 4 illustrate the absorption spectrum at this temperature as well as the corresponding deconvolution of the spectrum. In addition to showing the expected narrowing of the F_2^+** and F_2^+**-like color centers and increased absorption coefficients, it shows the presence of zero-phonon lines on both the high- and low-frequency tails of the large F_2 center's peak. Also, note the appearance of a new absorption peak with absorption maximum at $\nu_0 \approx 6\times 10^{14}$ Hz.

Table 2 shows the essential absorption data of the two F_2^+**-like centers at low temperature.

Much of the deconvolution data were available using information from the well-known papers by

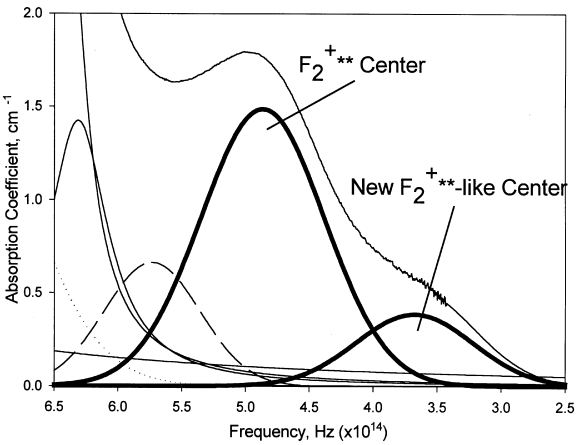

Fig. 2. Frequency range of F_2^+**-like color centers at 300 K.

Table 1
Absorption data at 300 K

$LiF:F_2^+$**	$LiF:F_2^+$**-like
$\nu_0 = 4.9\times 10^{14}$ Hz ± 2%	$\nu_0 = 3.7\times 10^{14}$ Hz ± 2%
$\Delta\nu = 3819\,cm^{-1}$	$\Delta\nu = 3591\,cm^{-1}$
$k_0 = 1.49\,cm^{-1}$	$k_0 = 0.38\,cm^{-1}$

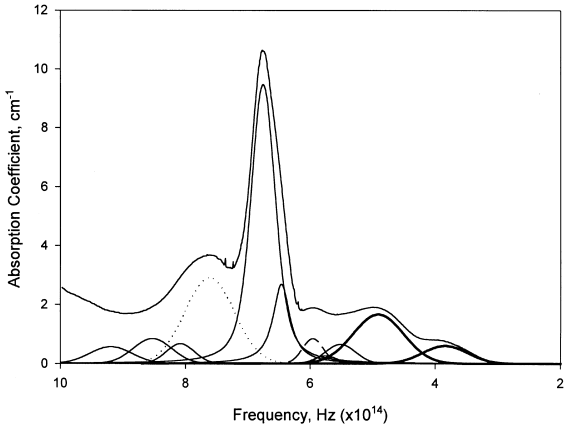

Fig. 3. Absorption spectrum and color center deconvolution at 13 K.

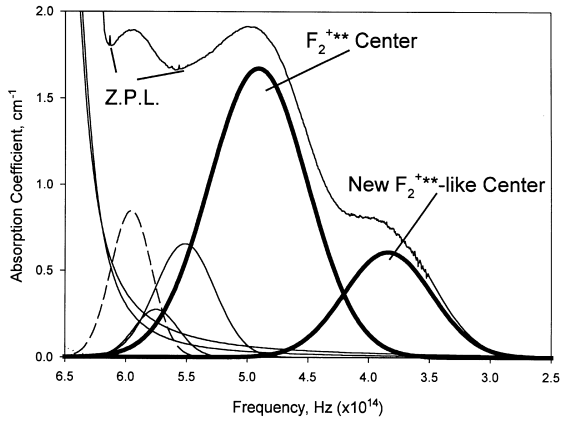

Fig. 4. Frequency range of F_2^+**-like color centers at 13 K.

Nahum [4,5]. Also, in agreement with Ref. [3], there were no zero-phonon lines detected for either the F_2^+** or F_2^+**-like color centers down to 13 K; however, experiments are currently being performed to study the effective phonon frequency of these centers using Resonance Raman scattering. Farge and Fontana performed similar investigations in [6] on standard F_2^+ color centers in LiF. Determination of these data will provide the final information to characterize both of these F_2^+**-like centers in this crystal with this particular dopant concentration.

Following transmission measurements, experiments of the fluorescence spectra were performed

Table 2
Absorption data at 13 K

LiF : F_2^+**	LiF : F_2^+**-like
$v_0 = 4.9\times10^{14}$ Hz ± 2%	$v_0 = 3.8\times10^{14}$ Hz ± 2%
$\Delta v = 3183\,cm^{-1}$	$\Delta v = 2834\,cm^{-1}$
$k_0 = 1.66\,cm^{-1}$	$k_0 = 0.61\,cm^{-1}$

using several different excitation wavelengths and several different sample temperatures. The excitation wavelengths include 532, 633, 747, 760, and 780.35 nm provided by the second harmonic of a Q-switched Nd : YAG, the Raman-shifted (D_2) second harmonic of the Q-switched Nd : YAG, Alexandrite (747 and 760 nm), and second harmonic of a Raman-shifted (D_2) fundamental frequency of Q-switched Nd : YAG lasers, respectively. Temperature varied from room temperature down to 13 K. The fluorescence radiation was collected by a fiber optic bundle and directed into an Acton Research ARC-750 (0.75 m) spectrometer. The detectors used were an Acton Research InGaAs detector (ID-441-C), which covers the spectral region from 800–1700 nm, and photomultiplier tube (PD-439, Model R406) sensitive from 400–1100 nm. The entire detection system was calibrated using a tungsten halogen lamp (Oriel Instruments Model 9-205) with known spectral output.

The following set of figures demonstrates the results of the fluorescence spectrum measurements. Each data set represented in the figures is corrected for the detection system; also, both Figs. 5 and 6 were performed at room temperature.

The interesting feature to notice is that the fluorescence spectra, measured under 532 and 633 nm excitation, are identical. However, when the same sample is excited by 760 nm light, the deconvolution of the total fluorescence reveals two fluorescing centers: the dominant fluorescence peak is identical to that found by 532 and 633 nm excitation and a smaller fluorescence band centered near 1080 nm (±10 nm). This is due to the presence of the new F_2^+**-like color center seen in the absorption spectrum deconvolution. In the case of 532 and 633 nm excitation, only the standard F_2^+** color center is being excited; however, at RT, light from the Alexandrite laser

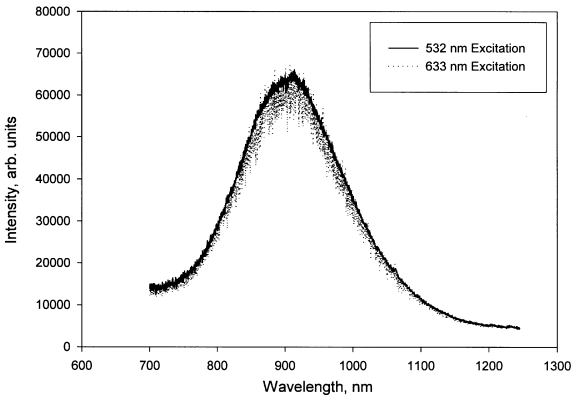

Fig. 5. Fluorescence spectra under 532 and 633 nm excitation at 300 K.

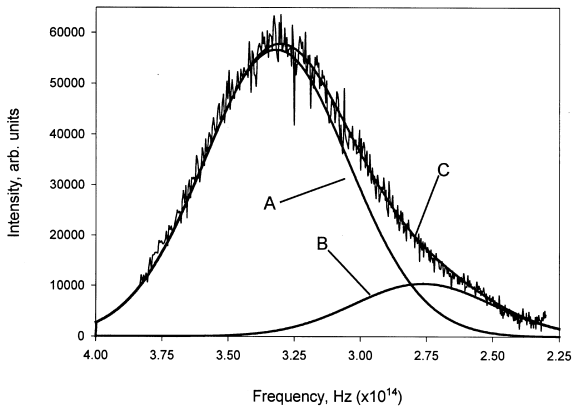

Fig. 6. Fluorescence spectra under 760 nm excitation at 300 K. (A) Emission from F_2^+**; (B) emission from new F_2^+**-like center; and (C) integral fluorescence spectrum and fitted curve.

at 760 nm is absorbed by both types of the centers. Therefore, we see that the fluorescence shown in Fig. 6 is due to both standard F_2^+** centers (predominantly) and the new F_2^+**-like centers. Table 3 shows the values determined by deconvolution of the fluorescence spectra at RT.

At lower temperatures, the fluorescence was measured using 747 and 760 nm from the Alexandrite laser.

Fig. 7 depicts these two spectra in which the 747 nm excitation beam causes fluorescence from both the standard F_2^+** centers as well as the new type of F_2^+** centers (predominant at this temperature and excitation wavelength).

Table 3
Fluorescence data at RT and 13 K

Temperature	LiF : F_2^+**	LiF : F_2^+**-like
300 K	Gaussian line shape $\lambda_0 = 906$ nm FWHM = 2174 cm^{-1}	Gaussian line shape $\lambda_0 = 1085$ nm FWHM = 2274 cm^{-1}
13 K	Gaussian line shape $\lambda = 898$ nm FWHM = 1515 cm^{-1}	Gaussian line shape $\lambda = 1080$ nm FWHM = 1657 cm^{-1}

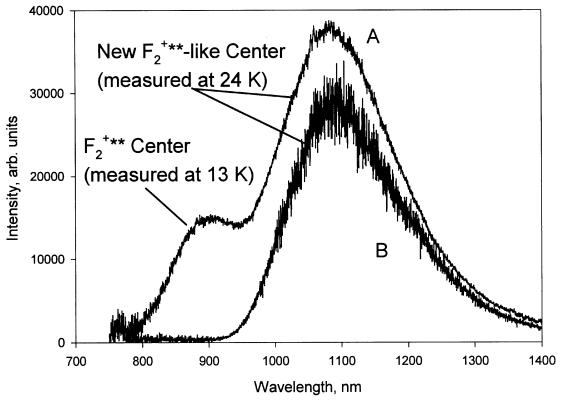

Fig. 7. Fluorescence under (A) 747 nm excitation at 24 K and (B) 760 nm excitation at 13 K.

It is also apparent from Fig. 7 how the two types of centers have narrowed with decreased temperature: RT excitation at 760 nm shows both centers fluorescing, while at 13 K standard F_2^+** is no longer being excited.

The final spectroscopic measurement required is the kinetics measurement to determine the lifetime of each of these centers. Fig. 8 shows the lifetime of standard F_2^+** centers under excitation from 532 and 633 nm at both RT and 13 K.

The exponential curves found in Fig. 8 describe the lifetimes as (A) $\tau = 32$ ns, (B) and (C) $\tau = 21$ ns, which results in a fluorescence quantum efficiency of $\eta = 66\%$.

Fig. 9 shows both the kinetics data of the new F_2^+**-like center, measured at 1100 nm, and the temporal profile of the excitation beam. The temporal response of our detection system, in this case a Electro-Optics Technology, Inc. amplified silicon detector (ET-2030A), was ~ 400 ps.

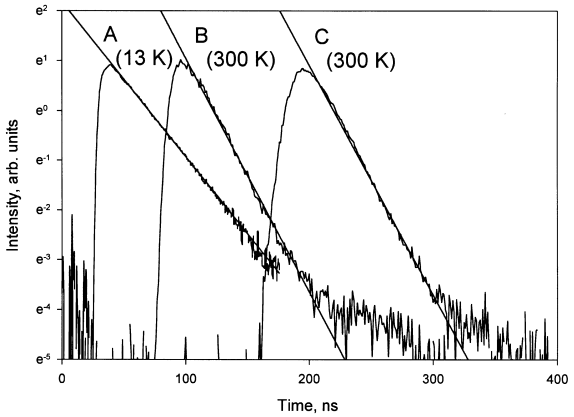

Fig. 8. Kinetics of fluorescence for F_2^+** centers at (A) 633 nm excitation, $T = 13$ K; (B) 633 nm excitation, $T = 300$ K; and (C) 532 nm excitation, $T = 300$ K.

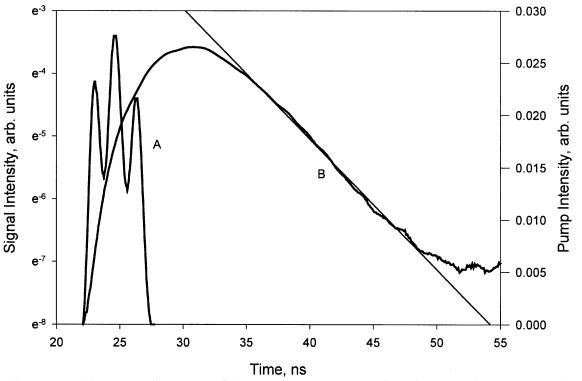

Fig. 9. (A) Top-hat profile, 780.35 nm excitation pulse (~ 4 ns) and (B) kinetics of fluorescence of new F_2^+**-like centers at 13 K.

The pump beam was the second harmonic of a Raman shifted (D_2) fundamental frequency of Nd : YAG with wavelength $\lambda = 780.35$ nm. Due to two nonlinear processes involved in the formation of the excitation pulse, it exhibits very fast rise and decay time with FWHM of 4 ns, as well as some fringe effects at its top. The figure clearly illustrates that the pulse duration of the excitation beam is not a factor when determining the lifetime of the F_2^+**-like center because the excitation pulse has already terminated while the fluorescence signal is still in the process of developing.

Because we found that the lifetime of this center was of the order of 5 ns at 13 K, we have been able to affirm that this center is not F_2^- nor F_3^-. Also supporting this, we found no zero-phonon line at 1040 nm as would be present if this new fluorescence was indeed that of F_2^-. The spectroscopic information for F_3^- is also well documented and it is clear that these centers are not present in our sample.

Further experiments have been performed to confirm the positive ionic charge of the new centers with absorption maximum at $\lambda = 808$ nm. In these experiments, two identical crystal samples of thickness, $t = 0.85$ cm, were measured at RT for transmission. One of the crystals was cooled to liquid nitrogen temperature (LNT) and re-irradiated with a dose of 5×10^3 rad using a ^{137}Cs source. LNT is lower than the temperature of hole-mobility in this crystal; also, the re-irradiation at LNT with a dose four orders of magnitude smaller than the original one used for preparation of the crystal does not create new centers in the crystal. By means of freezing the hole processes, the re-irradiation process selectively stimulates only recharging of existing centers by trapping free electrons. In other words, the LNT freezes the positively charged holes while the re-irradiation liberates trapped electrons, which then redistribute themselves among the various color centers present in the crystal. Positively charged centers then trap electrons, thereby reducing the center's absorption coefficient. Neutral centers will also trap electrons and subsequently increase the concentrations of negatively charged centers. Both irradiated and non-irradiated samples were measured for transmission at LNT and compared. The experiments conclude that the new centers ($\lambda_{abs} = 808$ nm) have essentially negligible absorption coefficients after re-irradiation at LNT and, therefore, must be positively charged centers.

3. Results and analysis

Given the spectroscopic data found thus far, we may make some calculations to determine the cross-sections of absorption and emission for both centers in these samples. The common expression

for the absorption cross-section, Eq. (1), is modified here for color center evaluation as is shown in Ref. [7].

$$\sigma_{\text{abs}} = \frac{c^2 A_{21} v_{\text{abs}}^0}{8\pi (v_{\text{fl}}^0)^3} \frac{2}{\Delta v} \sqrt{\frac{\ln 2}{\pi}}. \quad (1)$$

In Eq. (1), c is the speed of light in the medium ($n = 1.39$), A_{21} is the Einstein coefficient of spontaneous emission, v^0 is the central frequency of absorption/emission, and Δv is the half-width of the absorption band. Substituting in the values obtained for F_2^+** we can determine that the maximum value of the absorption cross-section is

$$\sigma_{\text{abs}}^0 = 1.24 \times 10^{-16}\ \text{cm}^2$$

The fluorescence cross-section can be calculated with the well-known formula

$$\sigma_{\text{fl}}^0 = \frac{c^2 A_{21}}{8\pi (v_{\text{fl}}^0)^2} \frac{2}{\Delta v} \sqrt{\frac{\ln 2}{\pi}}. \quad (2)$$

By evaluating this equation for known values, we obtain the maximum fluorescence cross-section as

$$\sigma_{\text{fl}}^0 = 1.48 \times 10^{-16}\ \text{cm}^2.$$

Fig. 10 illustrates the cross-section relationship of the F_2^+** color center at RT as a function of frequency.

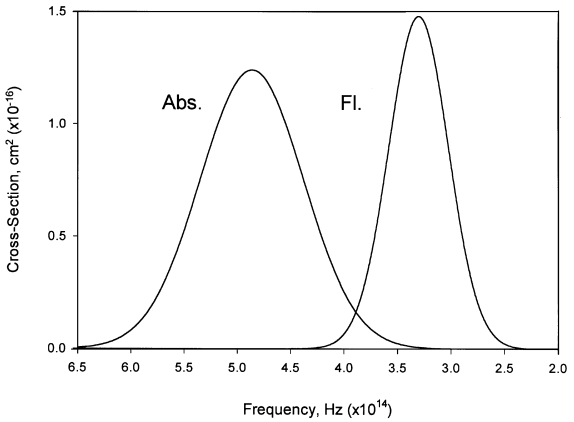

Fig. 10. Room temperature cross-sections of F_2^+** color centers.

4. Conclusions and future work

Using the spectroscopic data found within this study, we are performing calculations, which will optimize the cavity requirements to produce an ultrabroadband laser, much like the one described in Ref. [8], using this active medium. Using a novel laser cavity and proper pump wavelength, this medium should provide laser radiation over nearly its entire fluorescence spectrum from 800 to nearly 1300 nm at RT. To our knowledge, no other single laser medium has this large range of tunability.

Ref. [8] shows output efficiency for narrowband lasing and superbroadband lasing from $LiF:F_2^-$ as nearly equal. Similarly, it is expected that the efficiency of $LiF:F_2^+$** operating in superbroadband regime [9] will have comparable efficiency as is presented for narrowband lasing in Ref. [2].

Ultimately, this ultrabroadband laser will undergo a second-harmonic conversion of superbroadband infrared radiation into the visible spectral region from 400 to nearly 650 nm, providing a true white-light laser.

Also, investigations into modifying the crystal growth and annealing processes are being studied to enhance the production of both F_2^+** and F_2^+**-like color centers in the host medium, while at the same time limiting the production of other centers (F_2, F_3^+, etc.) that would serve as loss mechanisms in a laser using this medium.

It is our belief that this work, and the subsequent realization of an ultrabroadband, room-temperature stable laser based on this color center medium, will renew interest in color center crystals within the laser community as an excellent source of tunable laser radiation.

References

[1] S.B. Mirov, A.Yu. Dergachev, Powerful, room-temperature stable $LiF:F_2^+$** tunable laser, Proceedings of SPIE Vol. 2986, 1997, pp. 162–173.
[2] A.Yu. Dergachev, S.B. Mirov, Opt. Commun. 147 (1998) 107.
[3] V.V. Ter-Mikirtychev, J. Phys. Chem. Solids 58 (6) (1997) 893.
[4] J. Nahum, D.A. Wiegand, Phys. Rev. 154 (3) (1967) 817.
[5] J. Nahum, Phys. Rev. 158 (3) (1967) 814.

[6] Y. Farge, M.P. Fontana, Solid State Commun. 10 (1972) 333.
[7] Yu.E. Perlin, B.S. Tsukerblat, Effects of electron-vibrational interaction in optical spectra of paramagnetic impurity ions, Kishinev, Shtiintsg, 1974, pp. 1–368.
[8] T.T. Basiev, P.G. Zverev, V.V. Fedorov, S.B. Mirov, Appl. Opt. 36 (12) (1997) 2515.
[9] N.W. Jenkins, S.B. Mirov, V.V. Fedorov, Powerful, ultrabroadly tunable $LiF:F_2^{+**}$ laser, Proceedings of SPIE, Vol. 3929, 2000, pp. 278–288.